Inorg. Chem. **2006**, *45*, 8126–8135

Structural–Electronic Correlation in the First-Order Phase Transition of $[FeH_2L^{2-Me}](ClO_4)_2$ (H_2L^{2-Me} = Bis[((2-methylimidazol-4-yl)methylidene)-3-aminopropyl]ethylenediamine)

Nicolas Bréfuel,*,† Shinya Imatomi,† Haruna Torigoe,† Hiroaki Hagiwara,† Sergiu Shova,‡ Jean-François Meunier,§ Sébastien Bonhommeau,§,# Jean-Pierre Tuchagues,§ and Naohide Matsumoto*,†

Department of Chemistry, Faculty of Sciences, Kumamoto University, Kurokami 2-39-1, Kumamoto 860-8555, Japan, Institute of Applied Physics, Academy of Sciences of Moldova, Academiei str. 3. 2028 Chisinau, Moldova, Laboratoire de Chimie de Coordination, UPR 8241 CNRS, 205 Route de Narbonne, F-31077 Toulouse Cedex, France, and Laboratoire de Physique des Solides de Toulouse, UMR 5477 CNRS, 118 Route de Narbonne, F-31062 Toulouse Cedex, France

Received April 20, 2006

The synthesis and detailed study of the new mononuclear spin crossover complex $[Fe^{II}H_2L^{2-Me}](ClO_4)_2$ (where H_2L^{2-Me} = bis[((2-methylimidazol-4-yl)methylidene)-3-aminopropyl]ethylenediamine) are reported. Variable-temperature magnetic susceptibility measurements show the occurrence of a steep spin crossover centered at 171.5 K with a hysteresis loop of ca. 5 K width ($T_{1/2}^{\uparrow}$=174 K and $T_{1/2}^{\downarrow}$ = 169 K, for increasing and decreasing temperatures, respectively). The crystal structure has been resolved for the high-spin (HS) and low-spin (LS) states at 200 and 123 K, respectively, revealing a crystallographic phase transition that occurs concomitantly to the spin crossover: at 200 K, the complex crystallizes in the monoclinic system, space group $P2_1/n$, while the space group is $P2_1$ at 123 K. The mean Fe–N distances are shortened by 0.2 Å, but the thermal spin crossover is accompanied by significant structural changes: the rearrangement of the central atom C12 of a six-membered chelate ring of $[Fe^{II}H_2L^{2-Me}]^{2+}$ to two positions (C12A and C12B) and, consequently, the lack of an inversion center at 123 K ($P2_1$ space group). Both HS and LS supramolecular structures involve all possible hydrogen bonds between imidazole and amine NH functions, and perchlorate anions; however, the HS supramolecular structure is a one-dimensional (1D) network, and the LS phase may better be described as a two-dimensional (2D) extended structure of A and B molecules. The structural phase transition of $[FeH_2L^{2-Me}](ClO_4)_2$ seems to trigger the steep and hysteretic spin crossover. Discontinuities in the temperature dependence of the Mössbauer parameters (isomer shift and quadrupole splitting) at the spin crossover temperature confirmed the occurrence of a structural phase transition. The experimental enthalpy and entropy variations were determined by differential scanning calorimetry (DSC) as 7.5 ± 0.4 kJ/mol and 45 ± 3 J K^{-1} mol^{-1}, respectively. The regular solution theory was applied to the experimental data, yielding an interaction parameter of Γ = 3.36 kJ/mol, which is larger than $2RT_{1/2}$, which fulfills the condition for observing hysteresis.

Introduction

The spin crossover (SCO) phenomenon between low-spin (LS) and high-spin (HS) electronic states is among the most fascinating electronic structure phenomena in coordination chemistry.[1] Because of its theoretical and experimental aspects, as well as its potential applications,[2] this phenomenon has aroused intense research over the past decades. While SCO can be observed for d^4–d^7 transition-metal complexes, most attention has been focused on iron(II) complexes with nitrogen donor atoms (FeN_6 core), because of the easy triggering of their molecular bistability (HS, S = 2, $^5T_2 \leftrightarrow$ LS, S = 0, $^1A_1$) by temperature,[1] pressure,[3] or

* To whom correspondence should be addressed. Fax: +81-96-342-3390. E-mail addresses: nicolasbrefuel@yahoo.fr, naohide@aster.sci.kumamoto-u.ac.jp.
† Kumamoto University.
‡ Academy of Science of Moldova.
§ Laboratoire de Chimie de Coordination, Toulouse.
# Laboratoire de Physique des Solides de Toulouse.

10.1021/ic060674w CCC: $33.50
Published on Web 09/02/2006

light irradiation.[4] Moreover, many of these materials exhibit steep SCO with thermal hysteresis, affording interesting perspectives for the design of new molecular materials in the electronic technology area.[5] Such a magnetic behavior can be triggered by cooperative interactions between the active metal sites in the crystal, and two strategies have been developed: the polymeric approach,[6] where metal centers are covalently linked by chemical bridges, and the supramolecular approach, using intermolecular interactions in the crystal ($\pi-\pi$ stacking,[7] hydrogen bonding[8]). Moreover, few examples of first-order (hysteretic) SCO triggered by a structural phase transition have been reported.[9]

In this work, which is part of a project aimed at obtaining bulk-chiral iron(II) SCO materials to explore the possibility of achieving a magneto-chiral memory, we describe the detailed study of a new SCO material, $[Fe^{II}H_2L^{2-Me}](ClO_4)_2$. Although the hexadentate Schiff base ligand H_2L^{2-Me} (bis-[((2-methylimidazol-4-yl)methylidene)-3-aminopropyl]ethylenediamine; see Chart 1), which involves two terminal imidazole groups, is achiral, the resulting (isolated) complex molecule is chiral, because of the possible clockwise (Δ) or anticlockwise (Λ) wrapping of the ligand about the metal center. The magnetic susceptibility, differential scanning calorimetry (DSC), and X-ray analysis of the crystal structures in the HS (200 K) and LS (123 K) states are reported, as well as a detailed Mössbauer study. Special emphasis is dedicated to the structural phase transition concomitant to SCO that is evidenced by both X-ray and Mössbauer analyses. The experimental results are analyzed within the model of Slichter and Drickamer.[10]

Chart 1. Schematic Drawing of $[Fe^{II}H_2L^{2-Me}]^{2+}$

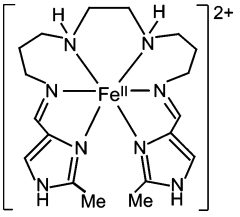

Experimental Section

Materials. All reagents and solvents used in this study are commercially available (Tokyo Kasei Co., Ltd. and Wako Pure Chemical Industries, Ltd.) and were used without further purification.

CAUTION! The perchlorate salts of metal complexes with organic ligands are potentially explosive. Only small quantities of the compound should be prepared, and it should be handled with great care!

Ligand. H_2L^{2-Me} was prepared aerobically via Schiff base condensation of *N*,*N*′-bis(3-aminopropyl)ethylenediamine (174 mg, 1 mmol) with 2-methyl-4-formylimidazole (220 mg, 2 mmol), in a 1:2 ratio, in 15 mL of ethanol. The freshly prepared pale yellow solution of the Schiff base ligand was deoxygenated by several nitrogen/vacuum cycles and used directly for iron complexation.

$[FeH_2L^{2-Me}](ClO_4)_2$. The synthesis of the iron(II) compound was performed in deoxygenated solvents under an inert atmosphere of N_2, using Schlenck techniques. $Fe(ClO_4)_2 \cdot 6H_2O$ (365 mg (1 mmol)) was dissolved in 15 mL of ethanol. This pale yellow solution was carefully degassed and added, through a cannula, to the H_2L^{2-Me} solution under stirring. The color of the solution changed quickly from pale yellow to red orange. After 10 min, the tiny amount of precipitate that had formed was filtered under nitrogen and the filtrate was partly evaporated (ca. 5 mL). The solution was allowed to stand overnight under a nitrogen atmosphere at room temperature, yielding orange crystals of $[FeH_2L^{2-Me}](ClO_4)_2$, which were collected by filtration, washed with ethanol, and dried under vacuum. Suitable single crystals were selected from this sample and used for the X-ray data collections. Yield: 350 mg (60%). Anal. Calcd for $C_{18}H_{30}N_8Cl_2O_8Fe$ (mw = 613.23 g/mol): C, 35.23; H, 4.64; N, 18.23. Found: C, 35.25; H, 4.93; N, 18.27. IR: $\nu_{C=N}$(imine), 1635 cm^{-1}; $\nu_{ClO_4^-}$, 1100, 1090 cm^{-1}.

Physical Measurements. Elemental analyses (C, H, N,) were performed at the Center for Instrumental Analysis of Kumamoto University by Miss Kikue Nishiyama. Infrared spectra were recorded on a Nicolet Avatar 370 DTGS (Thermo Electron

(1) See, for example: (a) Goodwin, H. A. *Coord. Chem. Rev*. **1976**, *18*, 293. (b) Gütlich, P. *Struct. Bonding (Berlin)* **1981**, *44*, 83. (c) König, E.; Ritter, G.; Kulshreshtha, S. K. *Chem. Rev.* **1985**, *85*, 219. (d) König, E. *Struct. Bonding (Berlin)* **1991**, *76*, 51. (e) Gütlich, P.; Hauser, A.; Spiering, H. *Angew. Chem.* **1994**, *106*, 2109; *Angew. Chem., Int. Ed. Engl*. **1994**, *33*, 2024. (f) Real, J. A.; Gaspar, A. B.; Niel, V.; Muñoz, M. C. *Coord. Chem. Rev*. **2003**, *235*, 121. (g) Gütlich, P.; Goodwin, H. A. In *Spin Crossover in Transition Metal* Compounds; Gütlich, P., Goodwin, H. A., Eds.; Topics in Current Chemistry, Vol. 233; Springer: New York, 2004; p 1. (h) Sorai, M.; Nakano, M.; Miyazaki, Y. *Chem. Rev*. **2006**, *106*, 976.

(2) (a) Kahn, O.; Martinez, C. J. *Science* **1998**, *279*, 44. (b) Hayami, S.; Danjobara, K.; Inoue, K.; Ogawa, Y.; Matsumoto, N.; Maeda, Y. *Adv. Mater*. **2004**, *16*, 869. (c) Létard, J. F.; Guionneau, P.; Goux-Capes, L. In *Spin Crossover in Transition Metal Compounds*; Gütlich, P., Goodwin, H. A., Eds.; Topics in Current Chemistry, Vol. 235; Springer: New York, 2004; p 221.

(3) Ksenofontov, V.; Gaspar, A. B.; Gütlich, P. In *Spin Crossover in Transition Metal Compounds*; Gütlich, P., Goodwin, H. A., Eds.; Topics in Current Chemistry, Vol. 235; Springer: New York, 2004; p 23.

(4) (a) Hauser, A. In *Spin Crossover in Transition Metal Compounds*; Gütlich, P., Goodwin, H. A., Eds.; Topics in Current Chemistry, Vol. 234; Springer: New York, 2004; p 155. (b) Bonhommeau, S.; Molnár, G.; Galet, A.; Zwick, A.; Real, J.-A.; McGarvey, J. J.; Bousseksou, A. *Angew. Chem.* **2005**, *117*, 4137; *Angew. Chem. Int. Ed.* **2005**, *44*, 4069.

(5) Kahn, O.; Launay, J. P. *Chemtronics* **1988**, *3*, 140.

(6) (a) Kröber, J.; Codjovi, E.; Kahn, O.; Grolière, F.; Jay, C. *J. Am. Chem. Soc.* **1993**, *115*, 9810. (b). Real, J. A., Gaspar, A. B.; Niel, V.; Muñoz, M. C. *Coord. Chem. Rev.* **2003**, *235*, 121.

(7) (a) Hayami, S.; Gu, Z.; Shiro, M.; Einaga, Y.; Fujishima, A.; Sato, O. *J. Am. Chem. Soc.* **2000**, *122*, 7126. (b) Hayami, S.; Gu, Z.; Yoshiki, H.; Fujishima, A.; Sato, O. *J. Am. Chem. Soc.* **2001**, *123*, 11644.

(8) (a) Sunatsuki, Y.; Ikuta, Y.; Matsumoto, N.; Ohta, H.; Kojima, M.; Iijima, S.; Hayami, S.; Maeda, Y.; Kaizaki, S.; Dahan, F.; Tuchagues, J.-P. *Angew. Chem.* **2003**, *115*, 1652; *Angew. Chem., Int. Ed.* **2003**, *42*, 1614. (b) Ikuta, Y.; Ooidemizu, M.; Yamahata, Y.; Yamada, M.; Osa, S.; Matsumoto, N.; Iijima, S.; Sunatsuki, Y.; Kojima, M.; Dahan, F.; Tuchagues, J.-P. *Inorg. Chem.* **2003**, *42*, 7001. (c)Yamada, M.; Ooidemizu, M.; Ikuta, Y.; Osa, S.; Matsumoto, N.; Iijima, S.; Kojima, M.; Dahan, F.; Tuchagues, J.-P. *Inorg. Chem.* **2003**, *42*, 8406. (d) Sunatsuki, Y.; Ohta, H.; Kojima, M.; Ikuta, Y.; Goto, Y.; Matsumoto, N.; Iijima, S.; Akashi, H.; Kaizaki, S.; Dahan, F.; Tuchagues, J.-P. *Inorg. Chem*. **2004**, *43*, 4154. (e) Arata, S.; Torigoe, H.; Iihoshi, T.; Matsumoto, N.; Dahan, F.; Tuchagues, J.-P. *Inorg. Chem.* **2005**, *44*, 9288.

(9) (a) Boinnard, D.; Bousseksou, A.; Dworkin, A.; Savariault, J.-M.; Varret, F.; Tuchagues, J.-P. *Inorg. Chem*. **1994**, *33*, 271 and references therein. (b) Guionneau, P.; Brigouleix, C.; Barrans, Y.; Goeta, A.; Letard, J.-F.; Howards, J. A. K.; Gaultier, J.; Chasseau, D. *C. R. Acad. Sci., Ser. IIc: Chim.* **2001**, *4*, 161; (c) Reger, D. L.; Little, C. A.; Young, V. G., Pink, M. *Inorg. Chem*. **2001**, *40*, 2870. (d) Jeftic, J.; Romstedt, H.; Hauser, A.; Goujon, A.; Codjovi, E.; Linares, J.; Varret, F. *Polyhedron* **2001**, *20*, 1599. (e) Chernyshov, D.; Hostettler, M.; Törnroos, K. W.; Bürgi, H.-B. *Angew. Chem., Int. Ed*. **2003**, *42*, 3825.

(10) Slichter, C. P.; Drickamer, H. G. *J. Chem. Phys.* **1972**, *56*, 2142.

Corporation), using KBr disks at room temperature. Magnetic measurements were performed on powdered samples using a MPMS5 SQUID susceptometer (Quantum Design), operating at a sweeping rate of 1 K/min with an applied field of 0.5 T, in the temperature range of 5−300 K. Experimental susceptibilities were corrected for the diamagnetism of the constituent atoms, using Pascal's constants.[11] Variable-temperature Mössbauer measurements were performed on a constant-acceleration conventional spectrometer with a 50 mCi source of ^{57}Co (Rh matrix) in the temperature range of 80−293 K, using a MD306 Oxford cryostat, with the thermal scanning being monitored by an Oxford ITC4 servo control device (±0.1 K). The absorber was a sample of ca. 100 mg of microcrystalline powder that was enclosed in a 20-mm-diameter cylindrical plastic sample holder, the size of which has been determined to optimize the absorption. The hyperfine parameters and their standard deviations of statistical origin (given in parentheses) were obtained by least-squares fitting to Lorentzian lines.[12] The isomer shift values (δ) are given with respect to metallic iron at room temperature. DSC measurements have been performed at a sweeping rate of 10 K/min, using a differential scanning calorimeter (Netzsch, model 204) on a ca. 10 mg powdered sample that was sealed in an aluminum pan with a mechanical crimp. Temperature and heat-flow calibrations were made with standard samples of indium, using its melting transition (429.6 K, 28.45 J/g). An overall accuracy of ±0.1 K in temperature and ±5% in heat capacity is estimated.

X-ray Crystallography. The selected orange block-shaped crystals of $[FeH_2L^{2-Me}](ClO_4)_2$ that were mounted readily shattered upon cooling below ∼170 K, and it was necessary to mount several crystals and cool them very slowly before succeeding to collect data of the LS phase. The X-ray diffraction (XRD) data were collected at 200 and 123 K with a Rigaku R-Axis Rapid diffractometer that was equipped with a cryosystem cooler device, using a graphite monochromator (λ = 0.71073 Å). The structures were solved by direct methods[13] and expanded using Fourier techniques.[14] The non-hydrogen atoms were refined anisotropically. At this stage, the subsequent Fourier difference syntheses revealed the positions of all H atoms. The H atoms were included in the final refinement using a riding model with U_{iso} = 1.2 U(atom of attachment). Neutral atom scattering factors were taken from Cromer and Waber.[15] Anomalous dispersion effects were included in F_c;[16] the values for $\Delta f'$ and $\Delta f''$ are those of Creagh and McAuley.[17] The values for the mass attenuation coefficients are those of Creagh and Hubbell.[18] All calculations were performed using the Crystal Structure software package.[19,20] A few residual peaks were located nearby O atoms that were bonded to Cl2 in the structure at 200 K (HS), indicating that this ClO_4^- anion is partially disordered. However, because of the low values of the corresponding electron densities, it was not possible to model this partial disorder. The molecular plots were obtained using the ZORTEP.[21] In the final full-matrix least-squares refinement, the function $[w(|F_o^2| - |F_c^2|)^2]^2$ was minimized. Crystal data and refinement details are given in Table 1.

Table 1. Summary of Crystal Data and Refinement Details for $[FeH_2L^{2-Me}](ClO_4)_2$

parameter	value	
	T = 123 K	T = 200 K
formula	$C_{18}H_{30}Cl_2FeN_8O_8$	$C_{18}H_{30}Cl_2FeN_8O_8$
formula weight	613.25	613.25
crystal system	monoclinic	monoclinic
space group	$P2_1$ (No. 4)	$P2_1/n$ (No. 14)
unit-cell parameters		
a	10.746(5) Å	11.268(3) Å
b	14.145(9) Å	14.023(4) Å
c	16.575(9) Å	16.443(4) Å
β	101.61(2)°	98.28(1)°
V	2468(2) Å^3	2571.1(12) Å^3
Z	4	4
ρ_{calcd}	1.651 Mg/m^3	1.584 Mg/m^3
λ	0.71073 Å	0.71073 Å
$\mu_{MoK\alpha}$	0.890 mm^{-1}	0.854 mm^{-1}
R^a [$I > 3\sigma(I)$]	0.0868	0.0457
wR^b	0.1972	0.1215

^{a} $R = ||F_o| - |F_c||/|F_o|$. ^{b} $wR = w(|F_o^2| - |F_c^2|)^2/ w|F_o^2|^2)]^{1/2}$.

The crystallographic data reported in Table 1 indicate that the crystal exhibits changes in the unit cell parameters upon HS → LS crossover, accompanied by a 25 Å^3/molecule decrease (4.2%) in the unit-cell volume. However, the most striking differences between the two structures consist in a change in space group between 200 K and 123 K; this structural phase transition is consistent with the above-mentioned observation that the crystals readily shattered upon cooling below ∼170 K. At 200 K, the space group was determined to be the centrosymmetric $P2_1/n$, whereas at 123 K, the crystal belongs to the subgroup $P2_1$ with two independent $[FeH_2L^{2-Me}](ClO_4)_2$ complex molecules in the unit cell. Examination of the systematic extinctions at 123 K has shown that there are 368 $h0l$ reflections and 37 reflections of which have intensities of $I > 3\sigma(I)$ and $h + l = 2n$. This systematic absence unequivocally agrees with the space group $P2_1$, indicating that, at 123 K, the n-plane and, consequently, the symmetry center are lacking. For the purpose of examining this situation, the structure at 123 K was also solved by assuming the $P2_1/n$ space group. This resulted in a structure that included one independent $[FeH_2L^{2-Me}](ClO_4)_2$ complex molecule where the C11−C12−C13 propyl group of the ligand seemed to be disordered over two positions with equal probabilities and the other atoms are normally determined, demonstrating that the conformational difference in the part of the C11−C12−C13 propyl group plays the key role in determining the space group. The 0.49(7) value of the Flack parameter indicates the presence of a twin via pseudo-inversion in the LS state.

Results

Magnetic Measurements. This sample exhibits a reversible change of color from yellow (HS) to deep red (LS),

(11) Kahn, O. *Molecular Magnetism*; VCH: Weinheim, Germany, 1993.
(12) Lagarrec, K. Recoil, Mössbauer Analysis Software for Windows. Available via the Internet at http:/www.physics.uottawa.ca/∼recoil.
(13) SIR92: Altomare, A.; Cascarano, G.; Giacovazzo, C.; Guagliardi, A.; Burla, M.; Polidori, G.; Camalli, M. *J. Appl. Crystallogr.* **1994**, *27*, 435.
(14) Beurskens, P. T.; Admiraal, G.; Beurskens, G.; Bosman, W. P.; de Gelder, R.; Israel, R.; Smits, J. M. M. DIRDIF99: The DIRDIF-99 program system, Technical Report of the Crystallography Laboratory, University of Nijmegen, The Netherlands, 1999.
(15) Cromer, D. T.; Waber, J. T. *International Tables for X-ray Crystallography*, Vol. IV; The Kynoch Press: Birmingham, England, 1974; Table 2.2 A.
(16) Ibers, J. A.; Hamilton, W. C. *Acta Crystallogr.* **1964**, *17*, 781.
(17) Creagh, D. C.; McAuley, W. J. *International Tables for Crystallography*, Vol. C; Wilson, A. J. C., Ed.; Kluwer Academic Publishers: Boston, 1992; Table 4.2.6.8, pp 219−222.
(18) Creagh, D. C.; Hubbell, J. H. *International Tables for Crystallography*, Vol. C; Wilson, A. J. C., Ed.; Kluwer Academic Publishers: Boston, 1992; Table 4.2.4.3, pp 200−206.
(19) CrystalStructure 3.6.0: Crystal Structure Analysis Package; Rigaku and Rigaku/MSC, 2000−2004, The Woodlands, TX.
(20) Watkin, D. J.; Prout, C. K.; Carruthers, J. R.; Betteridge, P. W. CRYSTALS, Issue 10; Chemical Crystallography Laboratory: Oxford, U.K., 1996.
(21) Zsolnai, L.; Pritzkow, H.; Huttner, G. ZORTEP. *Ortep for PC, Program for Molecular Graphics*; University of Heidelberg: Heidelberg, Germany, 1996.

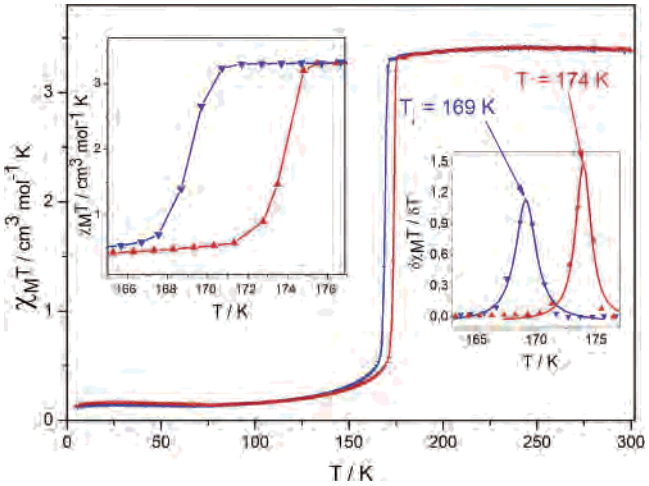

Figure 1. $\chi_M T$ vs T plot for the (▲) heating and (▼) cooling modes for $[FeH_2L^{2-Me}](ClO_4)_2$. The left and right insets represent a magnification of the hysteresis loop and the first derivative of $\delta\chi_M T/\delta T$, respectively.

suggesting a spin crossover. The sample was initially quickly cooled to 5 K within a few seconds, and the magnetic susceptibility was first measured in the heating mode from 5 K to 300 K, and then in the cooling mode from 300 K to 5 K. The magnetic behavior is very similar in the heating and cooling modes, except for the transition temperature, indicating the absence of a frozen-in effect. The thermal dependence of the product $\chi_M T$ is displayed in Figure 1, where χ_M is the molar magnetic susceptibility and T represents the temperature. The $\chi_M T$ value of 0.13 cm^3 K/mol at 5 K is slightly larger than the spin-only value that is expected for the d^6 LS state ($S = 0$), being compatible with those of LS iron(II) complexes. Upon warming from 5 K, $\chi_M T$ slowly increased up to 0.37 cm^3 K/mol at ca. 160 K, and then underwent a very sharp increase. The $\chi_M T$ value jumped up to 3.31 cm^3 K/mol at 175.5 K and then slowly increased up to ca. 3.40 cm^3 K/mol at 300 K, indicating a complete LS → HS SCO. This value, ca. 3.40 cm^3 K/mol, is slightly larger than the expected HS value ($S = 2$) and could indicate partial oxidation of the sample; however, the EPR spectra recorded at 295 and 100 K on a powdered sample did not show any absorption that was assignable to the Fe^{III} species. Upon subsequent cooling from 300 K, a similar behavior was observed for the HS → LS crossover. The critical temperatures for the heating ($T_{1/2}^{\uparrow}$) and cooling ($T_{1/2}^{\downarrow}$) modes (174 and 169 K, respectively) indicated the occurrence of a ca. 5 K wide thermal hysteresis characteristic of a first-order SCO.

DSC Measurements. The calorimetric measurements were performed in the temperature range of 150−190 K, at a sweeping rate of 10 K/min (Figure 2). The transition temperatures have been determined to be ca. 173 and 167 K, in the heating and cooling mode, respectively, indicating the occurrence of a 6-K-wide hysteresis. These values match those observed in the $\chi_M T$ vs T plot nicely. The overall enthalpy (ΔH) and entropy (ΔS) variations associated with this hysteretic SCO determined from the DSC curves are $\Delta H = -7.7 \pm 0.4$ kJ/mol and $\Delta S = -45 \pm 2$ J K^{-1} mol^{-1}, respectively, for the cooling mode and $\Delta H = 7.5 \pm 0.4$ kJ/mol and $\Delta S = 45 \pm 3$ J K^{-1} mol^{-1}, respectively, for the heating mode.

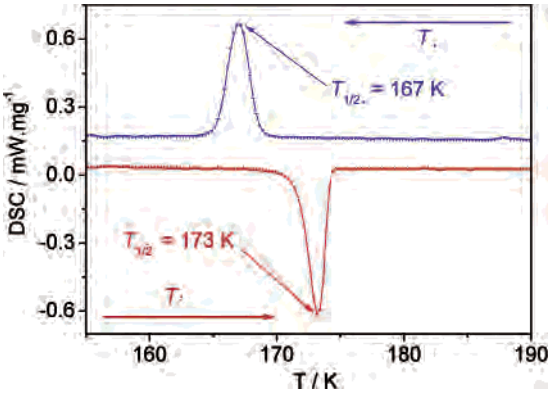

Figure 2. Differential scanning calorimetry (DSC) curves in the spin crossover (SCO) region for $[FeH_2L^{2-Me}](ClO_4)_2$; the blue and red curves correspond to the DSC data in the cooling and heating modes, respectively.

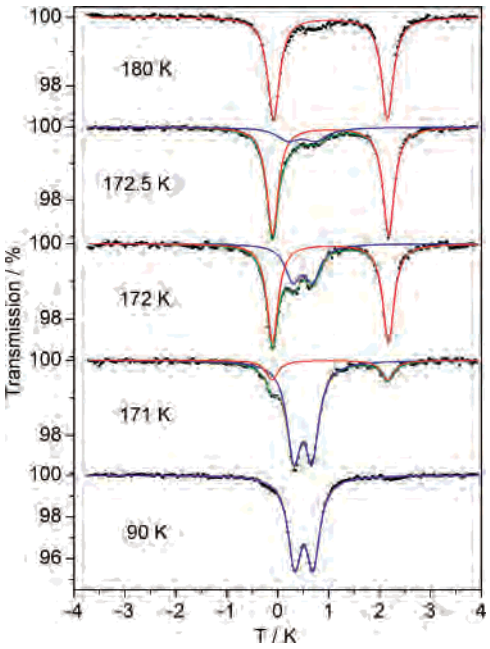

Figure 3. Selected ^{57}Fe Mössbauer spectra of $[FeH_2L^{2-Me}](ClO_4)_2$ recorded in the warming mode; the solid lines represent fitted curves with the parameters given in Table 2.

Mössbauer Spectroscopy. ^{57}Fe Mössbauer spectra of $[FeH_2L^{2-Me}](ClO_4)_2$ were recorded in the cooling and warming modes successively, varying the temperature very slowly between 293 K and 80 K, to avoid any hysteresis effect. Figure 3 shows representative spectra (recorded in the warming mode) clearly displaying the occurrence of a steep SCO centered at ca. 172 K.

The values of the Mössbauer parameters obtained by least-squares fitting are collated in Table 2. The low- and high-temperature spectra are characteristic of the LS and HS states of iron(II), respectively, with isomer shifts (δ) of 0.515(2) s^{-1} at 90 K and 1.035(2) mm s^{-1} at 200 K, and quadrupole splittings (ΔE_Q) of 0.363(4) mm/s at 90 K and 2.159(3) mm/s at 200 K. In the 160−173 K intermediate temperature range, the spectra consist of the LS and HS doublets in thermal equilibrium with each other. Small line broadenings are observed for the HS doublet at the lower end of the 160−

Table 2. Mössbauer Parameters of $[FeH_2L^{2-Me}](ClO_4)_2$ (from Spectra Collected in the Warming Mode)

	LS component			HS component			
temperature, T (K)	$\delta^{a,b}$	$\Delta E_Q{}^b$	$\Gamma^{b,c}$	$\delta^{a,b}$	$\Delta E_Q{}^b$	$\Gamma^{b,c}$	A_{HS} (%)
293				0.970(2)	1.849(3)	0.143(3)	
200				1.035(2)	2.159(3)	0.142(2)	
180				1.037(2)	2.235(4)	0.140(3)	
172.5	0.48(3)	0.55(3)	0.28(4)	1.039(2)	2.281(4)	0.134(3)	81(2)
172	0.49(2)	0.39(2)	0.18(4)	1.036(3)	2.277(5)	0.133(4)	68(2)
171	0.495(4)	0.355(5)	0.164(5)	1.02(2)	2.27(3)	0.15(2)	16(2)
169.5	0.496(4)	0.355(6)	0.162(5)	1.02(2)	2.28(4)	0.16(3)	13(3)
168	0.497(4)	0.359(4)	0.161(4)	1.02(2)	2.28(3)	0.14(2)	13(2)
167	0.501(3)	0.361(4)	0.165(4)	1.02(2)	2.29(3)	0.15(2)	13(2)
165	0.504(3)	0.361(4)	0.164(4)	1.03(2)	2.28(4)	0.17(3)	12(2)
163	0.503(3)	0.359(4)	0.167(4)	1.03(2)	2.30(4)	0.17(3)	12(2)
160	0.503(3)	0.363(4)	0.167(4)	1.03(2)	2.34(4)	0.15(3)	9(2)
150	0.504(3)	0.362(5)	0.167(4)				
125	0.508(3)	0.362(4)	0.163(4)				
105	0.509(2)	0.362(3)	0.160(3)				
90	0.515(2)	0.363(4)	0.156(3)				
80	0.515(2)	0.363(4)	0.156(3)				

[a] Isomer shifts are relative to iron foil. [b] Data expressed in units of mm/s. [c] Full width at half-height.

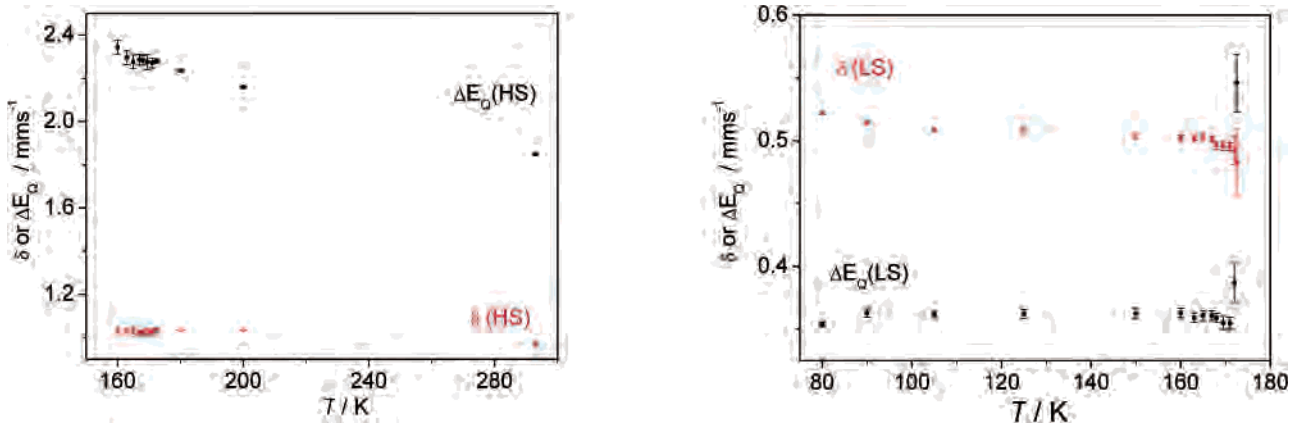

Figure 4. Temperature dependence of the isomer shift and quadrupole splitting of the HS (left) and LS (right) doublets of $[FeH_2L^{2-Me}](ClO_4)_2$. Errors bars represent statistical deviations.

173 K range, whereas those observed at the upper end of the 163−173 K range are more important and indicate that the LS ↔ HS conversion rates are of the order of magnitude of the hyperfine frequency (ca. 10^8 s^{-1}). The data in Figure 3 and Table 2 (see Supporting Information) clearly evidence a very steep SCO centered at 171.7 K (warming mode), which is in fair agreement with the magnetic (174 K) and DSC (173 K) results.

The residual HS fraction below 150 K is ∼4% and does not decrease anymore. On the other hand, the Mössbauer spectra above 173 K show a very weak (ca. 5%) and broad additional absorption between the two components of the HS doublet, closer to its low-velocity component. This very weak absorption is not observable at low temperature (in the velocity range identical to that of the LS component), therefore, it may originate either from the presence of a small residual LS fraction or from weak aerial oxidation of the Mössbauer sample. The low $\chi_M T$ value observed at 5 K (0.13 cm^3 K/mol) and the absence of EPR signal allow us to privilege the hypothesis of a residual LS fraction. Because the Mössbauer parameters of such very low residual fractions cannot be evaluated with confidence by fitting procedures, but do affect the accuracy of the parameters that characterize the major species, we have fitted the 80−150 K (LS) and the 180−293 K (HS) spectra both to one and two doublets, but selected the fits to one quadrupole split doublet. For the same reasons, the variations of the total area of the spectra (A_{tot}) and of the HS fraction (A_{HS}/A_{tot}) over the entire 80−293 K temperature range cannot be evaluated accurately; consequently, the Debye temperatures (Θ_D(LS) and Θ_D(HS)) cannot be approximated confidently.

The temperature dependence of the Mössbauer parameters has been plotted in Figure 4. δ(HS) and ΔE_Q(HS) show a tiny discontinuity around T_C, but δ(LS) and ΔE_Q(LS) exhibit larger discontinuities.

Crystal and Molecular Structure. Because $[FeH_2L^{2-Me}](ClO_4)_2$ exhibits a steep SCO at ca. 171.5 K [$^1/_2(T^{\downarrow}_{1/2} + T^{\uparrow}_{1/2})$], the single-crystal X-ray structure was determined in the HS (200 K) and LS (123 K) states. The unit-cell parameters reported in Table 1 evidence significant variations: a decreases when the temperature is reduced, while b and c increase. However, the most important change is the increase of β from 98.28(1)° to 101.61(2)°. The volume decrease of the unit cell upon HS to LS SCO is equal to 25 $Å^3$/molecule (4.2%): this variation results not only from thermal contraction of the crystal lattice, but also from contraction of the Fe−N distances upon SCO. Moreover,

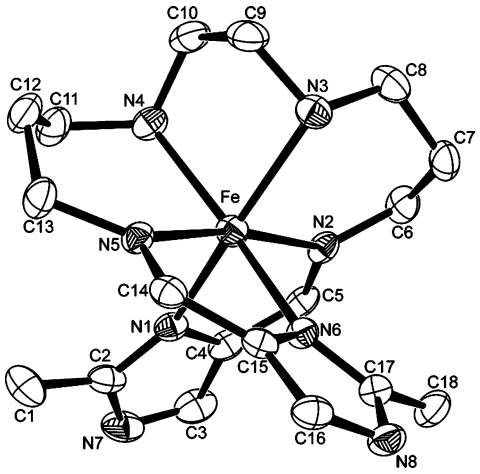

Figure 5. ORTEP drawing of $[FeH_2L^{2-Me}]^{2+}$ at 200 K with the atom numbering scheme. H atoms are omitted for clarity, and thermal ellipsoids are drawn at the 40% probability level.

the space group changes together with the spin-state: it is $P2_1/n$ in the HS state at 200 K and, it is $P2_1$ in the LS state at 123 K (see the Experimental Section).

At both temperatures, the crystal structure comprises $[FeH_2L^{2-Me}]^{2+}$ complex cations and ClO_4^- anions (1:2 ratio) that are associated through N−H···O bonds. At 200 K, the asymmetric unit for the $P2_1/n$ space group consists of one $[FeH_2L^{2-Me}]^{2+}$ complex cation and two ClO_4^- anions. Figure 5 shows an ORTEP drawing of the $[FeH_2L^{2-Me}]^{2+}$ complex cation at 200 K. The slightly distorted octahedral Fe^{II} coordination sphere includes six N atoms that belong to the linear hexadentate H_2L^{2-Me} ligand. As a consequence, three five-membered and two six-membered chelate rings alternate around the metal center.

At 123 K, the asymmetric unit for the $P2_1$ space group consists of two crystallographically independent Δ and Λ enantiomorphs, denoted as B and A, respectively. Figure 6 shows ORTEP drawings of molecules A and B with the atom numbering schemes. The Δ and Λ enantiomorphs are defined with respect to the axis joining the Fe atom to the middle of the C9−C10 bond. The helicoid N_6 ligand rotating along this axis moves the Λ enantiomorph A toward the observer

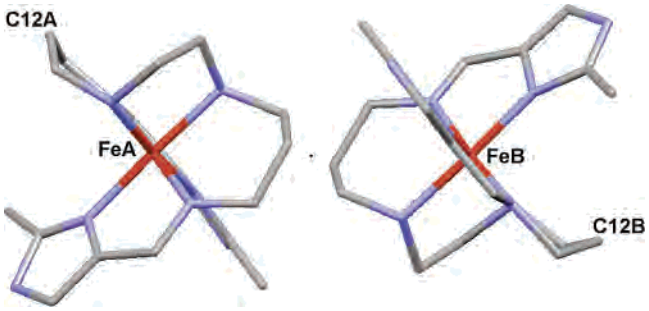

Figure 7. Pseudo-centrosymmetrically related enantiomorphs (molecule A (left) and molecule B (right)) of $[FeH_2L^{2-Me}](ClO_4)_2$ at 123 K. The C12A and C12B atoms of the six-membered chelate ring of Fe^{II} complex with the linear hexadentate ligand exclude the center of symmetry in the crystal packing of the complexes.

(right-hand molecule of Figure 6) while it moves the Δ enantiomorph B away from the observer (left-hand molecule of Figure 6). As a whole, the geometric characteristics of isomers A and B in the LS structure are very close to each other and are almost related by an inversion center; however, the conformation of the H_2L^{2-Me} ligand is different. This difference concerns the C11−C12−C13 propyl fragment of the ligand and results from the nonopposite orientation of atoms C12B and C12A (see Figure 7). This small difference leads to the lack of center of symmetry, being consistent with the $P2_1$ space group. The 0.49(7) value of the Flack parameter is also consistent with the presence of a twin by pseudo-inversion. The C12B position in the LS phase corresponds to the unique C12 position of the HS structure, and molecule A assumes a chair conformation at the six-membered chelate ring of −Fe−N4−C11−C12(A)-C13−N5−. As a result, although the −Fe−N4−C11−C12(A, B)−C13−N5− metallacycle has both the "chair" and "boat" conformations in the LS state, only the boat conformation of this metallacycle is retained in the HS isomer.

Table 3 shows the relevant coordination bond distances and angles for the HS and LS states. The average value of 2.202(3) Å for the metal-to-ligand bond lengths at 200 K is in good agreement with those observed for similar HS iron(II) complexes, whereas the values of 2.01(1) Å (A) and 2.00(1) Å (B), reported in Table 3, indicate that the Fe^{II} center is in

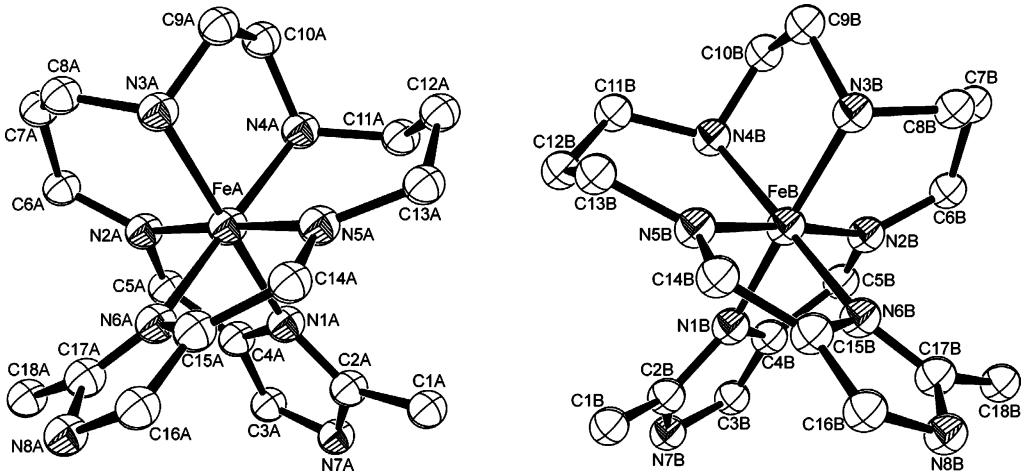

Figure 6. Drawing of the two independent $[FeH_2L^{2-Me}]^{2+}$ cations with the atom numbering scheme (△ enantiomorph (left) and Λ enantiomorph (right)) of the unit cell at 123 K.

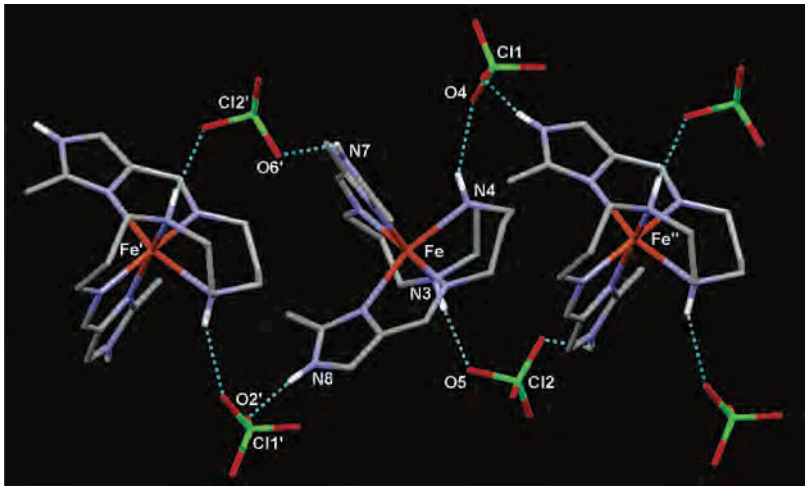

Figure 8. A hydrogen-bonded one-dimensional (1D) chain running along the *b*-axis in the crystal structure of $[FeH_2L^{2-Me}](ClO_4)_2$ at 200 K. Two adjacent Fe^{II} complexes are doubly bridged by two perchlorate anions. (Prime symbols denote the symmetry operations: $' = -x + 1/2, y + 1/2, -z + 1/2$; $'' = -x + 1, y - 1/2, -z$.)

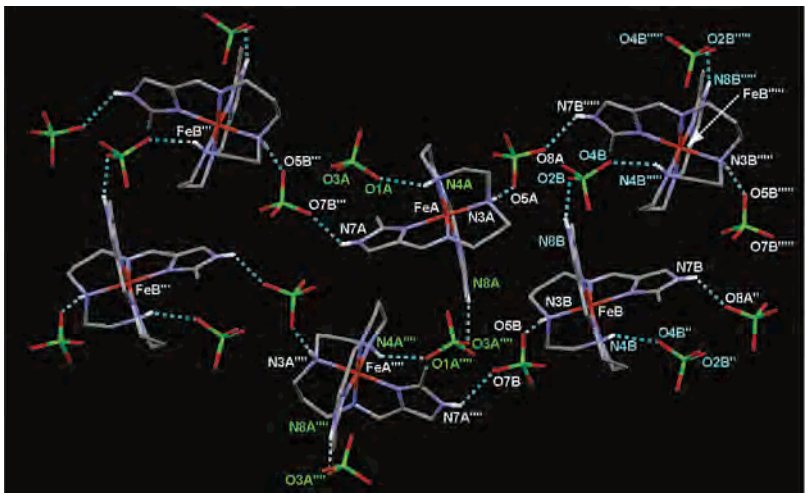

Figure 9. Two-dimensional (2D) supramolecular hydrogen-bond network in the crystal structure of $[FeH_2L^{2-Me}](ClO_4)_2$ at 123 K. In addition to the intrachain hydrogen bond, the interchain hydrogen bond produces a 2D network structure (symmetry operation: $'''' = -x, y + 1/2, 1 - z$).

the LS state at 123 K. It should also be mentioned that, upon HS → LS crossover, because of the contraction of the coordination sphere, the values of the N−Fe−N chelating angles get closer to those of a regular octahedron, by 4.9° on average.

Not only the space groups of $[FeH_2L^{2-Me}](ClO_4)_2$ are different—$P2_1/n$ (HS state, 200 K) and $P2_1$ (LS state, 123 K)—but also the crystal packing is different. In both cases, it essentially results from an extended network of intermolecular N−H···O bonds formed between both the imidazole and secondary amine N−H groups of the ligand and O atoms of the ClO_4^- anions. All hydrogen-bonding opportunities are realized in the crystal at 200 K as well as at 123 K; their geometric characteristics are presented in Table 4.

The crystal structure at 200 K can be described as a one-dimensional (1D) chain structure, as shown in Figure 8 and Table 4. Two adjacent complex cations are doubly bridged by two ClO_4^- anions through four N−H···O bonds to form a 1D structure, thus realizing all opportunities for hydrogen interactions. Note that, in the structure at 200 K, we did not take into account the N7−H···O7′ ($x - 1/2, 1/2 - y, 1/2 + z$) hydrogen interaction (N7−H = 0.86 Å, N7···O7′ = 2.986 Å, N7H···O7′ = 2.639 Å, ∠N7HO7′ = 105.5°), because, despite a reasonable N7···O7′ distance, the most relevant distance, N7H···O7′, is too large (2.639 Å), and, moreover, the 105.5° value for ∠N7HO7′ is too small. This is because H(N7) is not oriented toward O7′ ($x - 1/2, 1/2 - y, 1/2 + z$) but toward O6′ ($1/2 - x, 1/2 + y, 1/2 - z$). Accordingly, we considered the N7−H···O6′ ($1/2 - x, 1/2 + y, 1/2 - z$) hydrogen interaction, which has more reasonable metric parameters (N7−H = 0.86 Å, N7···O6′ = 3.103 Å, N7H···O6′ = 2.43 Å, ∠N7HO6′ = 135.2°) than the N7H···O7′ interaction.[22]

A similar system of intermolecular hydrogen bonds is responsible for the crystal packing at 123 K. However, at variance with the structure at 200 K, the 1D zigzag chains running along the *b*-axis are interconnected through weaker hydrogen interactions,[22] suggesting that the supramolecular structure of the LS phase may be described as a two-dimensional (2D) network structure. (See Figure 9.) Two adjacent complex cations within the 1D chain, molecule A

Table 3. Relevant Coordination Bond Distances and Angles in $[FeH_2L^{2-Me}](ClO_4)_2$ at 123 and 200 K

	$T = 123$ K		
pairing	molecule A	molecule B	$T = 200$ K
	Bond Distance (Å)		
Fe−N1	2.027(13)	1.953(14)	2.194(2)
Fe−N2	1.966(14)	2.021(13)	2.217(2)
Fe−N3	2.034(11)	1.996(13)	2.199(3)
Fe−N4	2.039(14)	2.047(16)	2.242(3)
Fe−N5	1.995(14)	1.944(14)	2.168(2)
Fe−N6	1.990(14)	2.034(15)	2.195(3)
	Bond Angle (deg)		
N2−Fe−N6	97.4(6)	96.9(6)	99.66(10)
N2−Fe−N5	177.8(6)	175.3(6)	168.84(9)
N6−Fe−N5	81.9(6)	81.8(5)	77.83(10)
N2−Fe−N1	82.1(6)	80.9(5)	76.94(10)
N2−Fe−N3	91.1(6)	93.7(5)	86.18(9)
N1−Fe−N3	172.5(5)	174.3(5)	161.76(9)
N2−Fe−N4	88.7(5)	88.0(6)	94.83(9)
N6−Fe−N4	173.1(6)	174.8(6)	164.31(10)
N5−Fe−N4	92.1(6)	93.5(6)	89.06(10)
N3−Fe−N4	84.7(5)	86.7(5)	79.66(10)

Table 4. Hydrogen-Bond Parameters for $[FeH_2L^{2-Me}](ClO_4)_2$ at 200 and 123 K

	Distance (Å)		
D−H···A[a]	D−H	H···A	angle D−H···A (deg)
	$T = 200$ K		
N4−H···O4	0.91	2.21	147.7
N7−H···O6′	0.86	2.43	135.2
N8−H···O2′	0.86	2.23	138.8
	$T = 123$ K		
N3A−H···O5A	0.91	2.21	172.5
N3B−H···O5B	0.91	2.17	168.3
N4A−H···O1A	0.91	2.39	144.4
N4B−H···O4B″	0.91	2.36	145.6
N7A−H···O7B‴	0.86	2.36	134.3
N3−H···O5	0.91	2.17	165.7
N7B−H···O8A″	0.86	2.38	130.9
N8A−H···O3A⁗	0.86	2.10	169.2
N8B−H···O2B	0.86	2.07	161.0

[a] Accent marks denote the various symmetry operations: ′: $-x + {}^1/_2, y + {}^1/_2, -z + {}^1/_2$; ″: $-x + 1, y - {}^1/_2, -z$; ‴: $-x, y + {}^1/_2, -z + 1$; ⁗: $-x, y - {}^1/_2, -z + 1$.

and B, are bridged by one ClO_4^- anion through NH(imidazole)···ClO_4···NH(secondary amine) hydrogen bonds. Thus, two among the four NH sites per molecule are used for the formation of a 1D chain. The remaining two NH sites are used for the interchain hydrogen bonds through the ClO_4^- anion, resulting a 2D network structure. However, although the zigzag chains including N3(A,B) and N8(A,B) involve hydrogen bonds that are sufficiently strong, the interchain hydrogen bonds including N4(A,B) and N7(A,B) involve weak hydrogen interactions.

Discussion

The presence of a pronounced 5-K-wide hysteresis, with a very steep SCO in both the heating and cooling modes observed by magnetic and calorimetric studies, evidences the first-order character of the spin-transition in $[FeH_2L^{2-Me}](ClO_4)_2$. In particular, it is remarkable that the LS ↔ HS conversion, as observed through thermal variation of the magnetic susceptibility, affects >80% of the molecules within a temperature range smaller than 2 K, both in the warming and cooling modes. The steep and hysteretic SCO is also observed by Mössbauer spectroscopy, not only through the presence of LS and HS doublets in thermal equilibrium with each other in a very narrow temperature range (163−173 K), but also through a significant increase in ΔE_Q(LS) above $T_{1/2}$, in agreement with the assumption that ΔE_Q(LS) is sensitive to intermolecular effects through the lattice contribution. The discontinuity observed in the thermal variation of δ(LS) is also associated with the occurrence of SCO. These significant variations are due to the fact that HS and LS molecules have different geometries, as evidenced by X-ray analysis, and these two crystallographic phases afford different lattice contributions.[9a,23]

The first-order spin-transition in $[FeH_2L^{2-Me}](ClO_4)_2$ is concomitant to a crystallographic phase transition, during which the monoclinic space group $P2_1/n$ of the HS state switches to its corresponding subgroup $P2_1$ in the LS state. Indeed, although a unique complex molecule is observed in the HS state, the X-ray analysis shows the presence of two distinct molecules in the LS phase, depending on the orientation of the propylene fragment of the ligand, and the presence of Δ and Λ enantiomorph molecules. The flexibility of the six-membered chelate ring of −Fe−N4−C11−C12-(A, B)-C13−N5- allows both the "chair" and "boat" conformations to have equivalent energies in the LS state. Upon SCO, the Fe−N distances exhibit significant lengthening (∼0.2 Å), inducing a more constrained structure, the strain of which is probably better released by the boat conformation of the six-membered chelate ring of the −Fe−N4−C11−C12−C13−N5− in the HS isomer.

The behavior of $[FeH_2L^{2-Me}](ClO_4)_2$ is quite unusual, because, at variance with previous examples, both LS and HS structures are ordered. For example, the DAPP ligand of [Fe(DAPP)(abpt)]$(ClO_4)_2$ (where DAPP = [bis(3-aminopropyl)(2-pyridylmethyl)amine] and abpt = 4-amino-3,5-bis-(pyridin-2-yl)-1,2,4-triazole) that has been described by Matouzenko et al.[24] exhibits an *order−disorder* transition when it converts from the LS state to the HS state: in the LS state, the propyl fragment of DAPP exhibits two distinct conformations, whereas an average conformation is observed in the HS state. The authors suggested that the presence of two ligand conformations may result in slightly different values of the HS−LS gap. Although the system can be "trapped" into the two possible conformations in the LS state,

(22) (a) Desiraju, G. R. *Acc. Chem. Res.* **1991**, *24*, 270. (b) Desiraju, G. R. *Acc. Chem. Res.* **1996**, *29*, 441. (c) Steiner, T. *Crystallogr. Rev.* **1996**, *6*, 1. (d) Steiner, T. *Chem. Commun.* **1997**, 727. (e) Jeffrey G. A. *An Introduction to Hydrogen Bonding*; Oxford University Press: New York, Oxford, 1997. (f) Desiraju, G. R.; Steiner, T. *The Weak Hydrogen Bond in Structural Chemistry and Biology*, Oxford University Press: New York, 2001. (g) Desiraju, G. R. *Chem. Commun.* **2005**, 2995.

(23) (a) Jeftić, J.; Romstedt, H.; Hauser, A. *J. Phys. Chem. Solids* **1996**, *57*, 1743. (b) Guionneau, P.; Létard, J. F.; Yufit, D. S.; Chasseau, D.; Bravic, G.; Goeta, A.; Howard, J. A. K.; Kahn, O. *J. Mater. Chem.* **1999**, *9*, 985. (c) Reger, D. L.; Little, C. A.; Young, V. G.; Pink, M. *Inorg. Chem.* **2001**, *40*, 2870. (d) Jeftić, J.; Matsarski, M.; Hauser, A.; Goujon, A.; Codjovi, E.; Linarès, J.; Varret, F. *Polyhedron* **2001**, *20*, 1599. (e) Money, V. A.; Elhaïk, J.; Radosavljevic Evans, I.; Halcrow, M. A.; Howard, J. A. K. *Dalton Trans.* **2004**, 65.

(24) Matouzenko, G. S.; Bousseksou, A.; Borshch, S. A.; Perrin, M.; Zein, S.; Salmon, L.; Molnár, G.; Lecocq, S. *Inorg. Chem.* **2004**, *43*, 227.

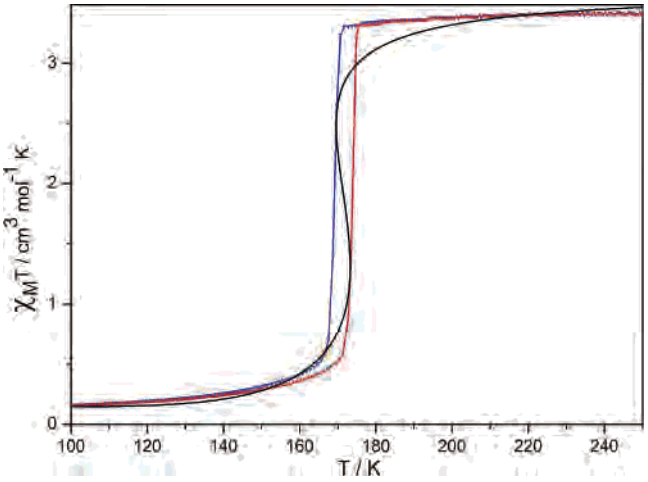

Figure 10. Numerical simulations of the magnetic behavior of $[FeH_2L^{2-Me}](ClO_4)_2$. The black line is the stationary states curve, with parameters of $\Delta H = 8.07$ kJ/mol, $\Delta S = 47$ J K^{-1} mol^{-1}, and $f_{HS} = 0.04$; the red and blue curves are the $\chi_M T$ vs T plots for the warming and cooling modes, respectively.

thermal energy allows quick interchange (crossing) between them, which results in the observation of an average position in the HS state. The unusual behavior of $[FeH_2L^{2-Me}](ClO_4)_2$, which exhibits an ordered HS structure, may be related to the hexadentate nature of the H_2L^{2-Me} ligand, which leads to a more constrained conformation than the tridentate DAPP ligand.

Moreover, the thermal SCO of $[FeH_2L^{2-Me}](ClO_4)_2$ is accompanied by a change not only in the lattice parameters, but also in the space group upon LS ↔ HS crossover (see Table 1). The crystal packing is also affected at the level of intermolecular interactions: a similar 1D network of Fe^{II} complex cations and perchlorate counteranions hydrogen-bonded into zigzag chains is present in both the HS and LS phases. However, additional weak hydrogen interactions interconnect the parallel 1D zigzag chains, which suggests that the LS phase may be better described as a 2D network.

Recently, we have described the synthesis and magnetic properties of a related compound $[FeHL^{2-Me}](ClO_4)$, in which $[HL^{2-Me}]^-$ denotes the mono-deprotonated form of the H_2L^{2-Me} ligand and the complex assumes an 1D zigzag chain structure, because of the intermolecular imidazolate−imidazole hydrogen bonds. This material exhibits a rather gradual SCO at ca. 165.5 K.[25] In the present case, the hexadentate H_2L^{2-Me} ligand provides a suitable ligand field strength for SCO, but it seems likely that the steepness of the first-order SCO in $[FeH_2L^{2-Me}](ClO_4)_2$ is related to the concomitant structural phase transition and the associated modification of the supramolecular structure.

The observed variation of entropy associated with SCO of 45 ± 3 J K^{-1} mol^{-1} is much larger than the entropy gain resulting from the $S = 0 \rightarrow S = 2$ change in spin-only value for iron(II) SCO systems ($R \ln 5 = 13.4$ J mol^{-1} K^{-1}). The reorientation of the propylene fragment (C12 atom) does not contribute to the overall entropy, because the structures in the HS and LS states are not disordered but fixed. The remaining amount can reasonably be attributed to the phonon entropy, resulting from the vibration modes of the $[FeN_6]$ core and intermolecular modes.[26]

Consistency between the magnetic and thermodynamic data has been examined using the regular solution model, which is expressed as follows:

$$\ln[(1 - \gamma_{HS})/(\gamma_{HS} - f_{HS})] = \frac{\Delta H + \Gamma(f_{HS} + 1 - 2\gamma_{HS})}{RT} - \frac{\Delta S}{R}$$

where ΔH and ΔS are the average values obtained from DSC measurements (cooling and warming modes) and Γ is the parameter that accounts for the cooperativity that is associated with SCO. γ_{HS} and f_{HS} are defined as $(\chi_M T)_T/(\chi_M T)_{HS}$ and $(\chi_M T)_{LT}/(\chi_M T)_{HS}$, respectively.[27] $(\chi_M T)_T$ is the value of $\chi_M T$ at any temperature, $(\chi_M T)_{HS}$ corresponds to the pure HS state, and $(\chi_M T)_{LT}$ corresponds to the value of $\chi_M T$ at low-temperature after the spin conversion has occurred. In the present case, $(\chi_M T)_{LT} = 0.13$ cm^3 K/mol ($f_{HS} \approx 0.04$). Figure 10 displays the corresponding steady-state curve (represented by the black line) computed using the aforementioned model. A satisfactory fit has been obtained by setting ΔH, ΔS, and f_{HS} to the experimental values (8.07 kJ/mol, 47 J K^{-1} mol^{-1}, and 0.04, respectively). Least-squares fitting leads to the interaction parameter $\Gamma = 3.36$ kJ/mol, which is larger than $2RT_{1/2}$ ($T_{1/2} = 171.5$ K) and fulfills accordingly the condition for observing hysteresis.[28]

Concluding Remarks

This work is part of a project whose objective is to obtain bulk-chiral iron(II) spin crossover (SCO) materials, to explore the possibility for achieving a magneto-chiral memory. Indeed, although the hexadentate Schiff base ligand is achiral, the resulting (isolated) complex is chiral, because of the possible clockwise (Δ) or anticlockwise (Λ) wrapping of the ligand about the metal center. However, in this specific case, the crystal packing is composed of adjacent complex molecules with different chirality, resulting in an achiral material in the bulk. Nevertheless, throughout this contribution, we have evidence that the $[FeH_2L^{2-Me}](ClO_4)_2$ compound exhibits an unusually steep SCO. The X-ray structure determinations showed that this first-order SCO is associated with a structural phase transition. The complex cation of this supramolecular material exhibits an unprecedented change, namely, the reversible rearrangement of one propylene group of the hexadentate ligand for half of the complex cations, concomitantly to the LS ↔ HS crossover. An investigation of the possible relationship between such a structural change and the magnetic properties of this material using density functional theory (DFT) calculations is underway. The structural and magnetic phase transition in $[FeH_2L^{2-Me}](ClO_4)_2$,

(25) Bréfuel, N.; Shova, S.; Tuchagues, J.-P.; Matsumoto, N. *Chem. Lett.* **2005**, *34*, 1092.

(26) (a) Tuchagues, J.-P.; Bousseksou, A.; Molnar, G.; McGarvey, J. J.; Varret, F. In *Spin Crossover in Transition Metal Compounds*; Gütlich, P., Goodwin, H. A., Eds.; Topics in Current Chemistry, Vol. 235; Springer: New York, 2004; p 85. (b) Sorai, M.; Seki, S. *J. Phys. Chem. Solids* **1974**, *35*, 555. (c) Sorai, M. *Pure Appl. Chem.* **2005**, *77*, 1331.

(27) Galet, A.; Munoz, M. C.; Gaspar, A. B.; Real, J. A. *Inorg. Chem.* **2005**, *44*, 8749.

(28) Honig, J. M. *J. Chem. Educ.* **1999**, *76*, 848.

which is characterized by a very steep SCO in both the heating and cooling modes with a 5-K-wide hysteresis, evidencing the first-order character of the spin-transition, is also observed by magnetic, calorimetric, and Mössbauer studies. A step forward in the study of this series of materials concerns the effect of the counter-anion on the bulk chirality as well as the SCO properties within the $[FeH_2L^{2-Me}]X_2$ family. This work currently has been undertaken.

Acknowledgment. This work was supported by a Grant-in-Aid (No. 16205010) from the Ministry of Education, Science, Sports and Culture, Japan. N.B. is grateful to the JSPS for providing Foreign Postdoctoral Fellowship. The authors are grateful to M. Sorai (Osaka University, Japan) and G. J. Long (University of Missouri−Rolla) for helpful discussions on calorimetry and Mössbauer spectroscopy.

Supporting Information Available: The Supporting Information includes crystallographic information files (CIF). This material is available free of charge via the Internet at http://pubs.acs.org.

IC060674W